International Journal of Nanomedicine

Dovepress
open access to scientific and medical research

Open Access Full Text Article

ORIGINAL RESEARCH

Combined Therapeutic Effects of ^{131}I-Labeled and 5Fu-Loaded Multifunctional Nanoparticles in Colorectal Cancer

This article was published in the following Dove Press journal:
International Journal of Nanomedicine

Pingping Wu[1,2]
Huayun Zhu[2]
Yan Zhuang[2]
Xiaofeng Sun[2]
Ning Gu[1]

[1]State Key Laboratory of Bioelectronics, Jiangsu Key Laboratory for Biomaterials and Devices, School of Biological Sciences and Medical Engineering, Southeast University, Nanjing 210096, People's Republic of China; [2]Department of Medical Oncology, Jiangsu Cancer Hospital & Jiangsu Institute of Cancer Research & The Affiliated Cancer Hospital of Nanjing Medical University, Nanjing 210009, People's Republic of China

Background: Owing to its combined effects, the co-delivery of different therapeutics is a promising option for the treatment of cancer. In the present study, tumor-targeting poly (ethylene glycol)-poly(lactic acid) (PEG-PLA) nanoparticles were developed for the transportation of two molecules, namely chemotherapeutic drug 5-fluorouracil (5Fu) and radionuclide iodine-131 (^{131}I), in a single platform.

Methods: The obtained nanoparticles (Cetuximab [Cet]-PEG-PLA-5Fu-^{131}I) were spherical (diameter approximately 110 nm) and pH-sensitive. The targeting effect of nanoparticles via Cet was confirmed in colorectal cancer cells using a fluorescent assay. The combined effects of Cet-PEG-PLA-5Fu-^{131}I on cell viability and apoptosis were evaluated in colorectal cancer cells by Cell Counting Kit-8 and flow cytometry assays.

Results: Blank nanoparticles (Cet-PEG-PLA) showed good biocompatibility, and Cet-PEG-PLA-5Fu-^{131}I nanoparticles were the most effective in terms of inhibition of cell viability and induction of apoptosis compared with monotherapy using Cet-PEG-PLA-5Fu or Cet-PEG-PLA-^{131}I. In the xenograft mouse model, compared with using Cet-PEG-PLA-5Fu or Cet-PEG-PLA-^{131}I alone, Cet-PEG-PLA-5Fu-^{131}I nanoparticles exhibited prolonged circulation in the blood and accumulation in the tumor, thus resulting in enhanced antitumor efficacy. Additionally, combined radio-chemotherapy with Cet-PEG-PLA-5Fu-^{131}I nanoparticles was associated with smaller tumor sizes than monotherapy, revealing the superior antitumor effects of Cet-PEG-PLA-5Fu-^{131}I nanoparticles. These effects were further evidenced by histological and immunohistochemical analyses.

Conclusion: The multifunctional Cet-PEG-PLA-5Fu-^{131}I nanoparticles are promising candidates for the co-delivery of 5Fu-mediated chemotherapy and ^{131}I-mediated radiotherapy.

Keywords: PEG-PLA, 5Fu, ^{131}I, drug delivery, radio-chemotherapy, colorectal cancer

Introduction

Colorectal cancer is the third most commonly diagnosed malignancy, accounting for 10% of all cancer cases worldwide.[1] Approximately 25% of the patients present with other metastatic disease, which develops in 50% of the newly diagnosed patients.[2] There are various therapeutic options for colorectal cancer, such as chemotherapy, radiotherapy, immunotherapy, and surgery.[3–5] However, monotherapy with chemotherapeutic drugs or radioactive isotopes is usually associated with inadequate therapeutic results because of its poor specificity and dose-dependent adverse effects.[6,7] Radiotherapy and chemotherapy strategies are commonly combined for the treatment of cancer in the clinic to achieve synergetic therapeutic outcomes.[8]

Correspondence: Ning Gu
State Key Laboratory of Bioelectronics, Jiangsu Key Laboratory for Biomaterials and Devices, School of Biological Sciences and Medical Engineering, Southeast University, Nanjing 210096, People's Republic of China
Tel +86 130 7253 2619
Email guning@seu.edu.cn

submit your manuscript | www.dovepress.com
DovePress
http://doi.org/10.2147/IJN.S215137

Radiotherapy has been utilized in anticancer treatment owing to its ability to kill tumor cells by damaging their DNA.[9] Various radionuclides, such as iodine-131 (^{131}I) can be bio-conjugated or loaded to nanoparticles resulting in improved therapeutic effects. Radionuclide ^{131}I, serving as a radiotherapy agent, provides imaging feasibility, as well as gamma- and beta-emitting treatment effects.[10] 5-fluorouracil (5Fu) is one of the most common chemotherapeutic drugs for the treatment of colorectal cancer.[11] However, the applications of 5Fu are limited by side effects due to non-specificity and short circulation half-life in the plasma.[12] Therefore, it could be expected that the loading of 5Fu to a targeted drug delivery system will optimize its therapeutic efficacy, due to a controlled delivery to the tumor tissue and optimization of the poor pharmacokinetic profile (eg, extensive biodistribution and short half-life).

Over the past few years, nanomedicine has exploited the potential of designing tumor-targeted nanocarriers which can deliver anticancer drugs in a molecule-selective manner, thereby improving the safety and efficacy of anticancer treatment.[13,14] Accumulating studies have demonstrated the feasibility of the application of tumor-targeted nanoparticles.[15,16] Nanotechnology has provided deep insights into the understanding of biological processes in diseases and enabled the development of novel therapeutics for the treatment of cancer.[17] Targeted drug delivery systems, especially active targeting nanoparticles, have been employed to improve the bioavailability and biodistribution of chemical agents.[18] The abundant expression of target molecules is mandatory for successful receptor-mediated tumor imaging and therapy. The epidermal growth factor receptor (EGFR), a transmembrane receptor located on the cell surface, plays a vital role in signaling pathways which regulate cell proliferation and tumor metastasis.[19] A previous study suggested that EGFR is highly expressed in different types of tumors, including colorectal cancer.[20] Hence, EGFR is a valuable candidate for the treatment of cancer. Cetuximab (Cet) is a monoclonal immunoglobulin G1 antibody that targets EGFR and suppresses the proliferation of different cancer cells.[21]

Poly(lactic acid) (PLA) has been utilized in various studies as a drug carrier owing to its biocompatibility and biodegradability.[22,23] However, its application is limited by high hydrophobicity and entrapment by macrophages, which results in undesired effects (eg, lower drug-loading capability and reduced drug-accumulating time).[24] Copolymerization with other polymers, particularly hydrophilic polymers such as poly(ethylene glycol) (PEG), may help address the shortcomings of PLA polymeric systems.[25] Different types of copolymers, such as methoxy PEG (mPEG)-PLA and mPEG-PLA-mPEG, which are characterized by core-shell structures, could be produced through copolymerization of PLA with PEG. Notably, Genexol-PM, a mPEG-PLA-based polymeric micelles product, has been marketed for cancer therapy.[26]

In this study, we constructed Cet-decorated multifunctional nanoparticles (Cet-PEG-PLA-5Fu-^{131}I) by loading 5Fu and ^{131}I to achieve combined radio-chemotherapy of colorectal cancer (Scheme 1). We firstly characterized the physical profiles of the obtained nanoparticles and their intracellular uptake. Subsequently, we investigated the in vivo blood circulation and distribution of the nanoparticles. Finally, we ascertained the combined antitumor activity

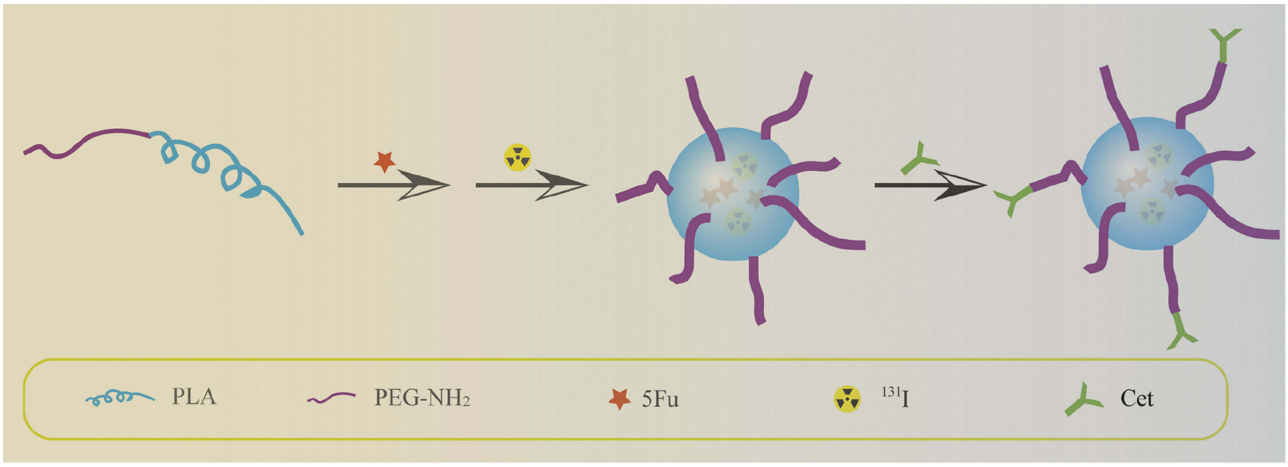

Scheme 1 The preparation of Cet-PEG-PLA-5Fu-^{131}I nanoparticles.

of the prepared nanoparticles in a colorectal cancer cell xenografted mouse model.

Materials and Methods

Materials

Amine-terminated PEG (molecular weight [MW]: 5 kDa) functionalized PLA (MW: 10 kDa) was procured from Daigang Bio-material (Jinan, China). 5Fu was obtained from Simcere Pharmaceutical Group (Nanjing, China). Radionuclide ^{131}I was purchased from Shanghai GMS Pharmaceutical Co., Ltd. (Shanghai, China). All other reagents were of analytical grade.

Preparation of Cet-PEG-PLA -5Fu-^{131}I Nanoparticles

Preparation of PEG-PLA-5Fu

The water-in-oil-in-water (w/o/w) solvent evaporation method was performed to fabricate the Cet-PEG-PLA-5Fu nanoparticles. Briefly, 10 mg of PEG-PLA was dissolved in 1 mL of trichloromethane and stirred at room temperature to obtain a uniform solution. 5Fu (2 mg) was dispersed in 0.2 mL of Millipore water, added to PLA solution, and sonicated at 200 W for 5 min to generate the w/o primary solution. The primary solution was centrifuged at 3,000 rpm to remove free 5Fu and PLA, and emulsified with 2 mL of 2% polyvinyl alcohol solution containing Tween 80 as a surfactant by rotating at 9,500 rpm for 30 min to generate the final w/o/w emulsion. Finally, the solution was evaporated to volatile trichloromethane at 30°C for 30 min.

Fabrication of PEG-PLA-5Fu-^{131}I and PEG-PLA-^{131}I

PEG-PLA-5Fu and PEG-PLA were labeled with ^{131}I via the chemical iodide method.[28] In brief, 200 μCi of ^{131}I was added into PEG-PLA-5Fu or PEG-PLA (10 mg/mL, 1 mL). Subsequently, the mixture was coated with iodogen followed by sonication for 5 min at 37°C. Free ^{131}I was removed by centrifugation using a filter (MW cut-off: 10 kDa) and washed until radioactivity was no longer detected. The radiolabeling yield of the labeled nanoparticles was evaluated using an automatic gamma counter (LKB gamma 1261; LKB Instruments).

Cet Decoration of Nanoparticles

Cet (0.5 mg) was added into the aqueous solution of PEG-PLA, PEG-PLA-5Fu, PEG-PLA-^{131}I, and PEG-PLA -5Fu-^{131}I (PEG-PLA concentration: 1 mg/mL) in the presence of 1-ethyl-3-(3-dimethylaminopropyl)carbodiimide hydrochloride and co-incubated under gentle stirring at room temperature for 6 h. Finally, Cet-decorated nanoparticles were generated by centrifugation at 10,000 rpm for 10 min.

Characterization of Nanoparticles

The hydrodynamic size and zeta potential of nanoparticles were detected by dynamic light scattering (DLS). The morphological characteristics of nanoparticles were observed through transmission electron microscopy (TEM). Cet-modified PEG-PLA nanoparticles were characterized using Fourier transform infrared (FTIR) and nuclear magnetic resonance (NMR) spectroscopy devices.

Loading and Release of 5Fu

The amount of 5Fu in the nanoparticles was detected using an ultraviolet–visible spectrophotometer. Lyophilized nanoparticles (1 mg) were dissolved in 1 mL of hydrochloric acid to extract 5Fu for loading and encapsulation measurement. The samples were gently shaken for 6 h at 95°C to completely leach out 5Fu. Following filtration, 100 μL of supernatant was diluted to 1 mL. The amount of 5Fu loaded and encapsulated in nanoparticles was measured using an ultraviolet–visible spectrophotometer at a wavelength of 265 nm. It was expressed as loading efficiency and encapsulation efficiency calculated as follows:

$$\text{Loading efficiency}\,(\%) = \frac{\text{Amount of 5Fu in nanoparticles}}{\text{Total weight of nanoparticles}} \times 100$$

$$\text{Encapsulation efficiency}\,(\%) = \frac{\text{Amount of 5Fu in nanoparticles}}{\text{Total amount of added 5Fu}} \times 100$$

The sustained release of 5Fu from nanoparticles was examined by dissolving 100 mg of nanoparticles in phosphate-buffered saline (PBS; pH 5.0 and 7.4). The solution (15 mL) was divided into 30 Eppendorf tubes, and the samples were placed in a shaker at 200 rpm at 37°C. At predetermined time intervals, each sample was withdrawn and prepared according to the aforementioned method. The absorbance of each released sample was calculated as follows:

$$\text{Accumulated release}\,(\%) = \frac{\text{Amount of 5Fu released}}{\text{Total amount of nanoparticles} \times \text{Loading efficiency}(\%)} \times 100$$

Radiolabeling Stability of ^{131}I-Labeled Nanoparticles

Cet-PEG-PLA-^{131}I or Cet-PEG-PLA-5Fu-^{131}I were added to fresh human serum and PBS for predetermined time intervals at 37°C to evaluate the stability of radionuclide ^{131}I. Serum samples (10 μL) were withdrawn and centrifuged to remove the detached radionuclide. Subsequently, the radioactivity was examined using an automatic gamma counter (LKB gamma 1261; LKB Instruments).

Cellular Uptake of Nanoparticles

The fluorescent dye indocyanine green (ICG) was encapsulated in Cet-PEG-PLA nanoparticles as a fluorescence probe for evaluating the uptake of the nanoparticles.[27] SW620 cells (Chinese Academy of Sciences, Shanghai, China) were cultured in a glass bottom dish at a density of 4×10^6 for 24 h. Cet-PEG-PLA-ICG and PEG-PLA-ICG were added and incubated for 30 min and 4 h at 37°C, respectively. Subsequently, the cells were treated with 4′,6-diamidino-2-phenylindole for 10 min and washed thrice with PBS. Images were captured under a confocal fluorescence microscope (Leica TCS SP8).

In vitro Cytotoxicity Assay

SW620 colorectal cancer cells were seeded in 96-well plates at a density of 5×10^4 cells/well and cultured in Dulbecco's modified Eagle's medium supplemented with 10% fetal bovine serum at 37°C. After 24 h, different concentrations of Cet-PEG-PLA, free 5Fu, ^{131}I, Cet-PEG-PLA-5Fu, Cet-PEG-PLA-^{131}I, and Cet-PEG-PLA-5Fu-^{131}I were added and incubated for another 24 h. Next, 10 μL of Cell Counting Kit-8 solution was added and the plates were incubated for 1 h.

Cell Apoptosis

Cells were seeded in a six-well plate at a density of 3×10^5 cells/well and incubated for 24 h. The old medium was replaced with new medium containing Cet-PEG-PLA-5Fu (5 μg/mL of 5Fu), Cet-PEG-PLA-^{131}I (200 μCi of ^{131}I), or Cet-PEG-PLA-5Fu-^{131}I (5 μg/mL of 5Fu, 200 μCi of ^{131}I). After incubation for 24 h, cells were trypsinized and resuspended in 300 μL of binding buffer. Subsequently, 5 μL of Annexin V-propidium iodide was added for 15 min and mixed with 200 μL of binding buffer. Finally, cells were analyzed using a flow cytometer (BD Biosciences, USA).

Animal Model

BALB/c mice (age: 6–8 weeks, weight: 18–22 g) were purchased from the Animal Center of Cancer Hospital Chinese Academy of Medical Sciences (Beijing, China) and housed under standard conditions. All animal procedures were performed in accordance with the Guide for the Care and Use of Laboratory Animals of the National Institutes of Health and approved by the Committee on the Ethics of Animal Experiments. SW620 cells (3×10^6) in 100 μL of PBS were subcutaneously injected into the right flank of mice to establish the xenograft model.

Blood Circulation and Biodistribution Study

Normal BALB/c mice were intravenously injected with free ^{131}I (200 μCi), Cet-PEG-PLA-^{131}I, and Cet-PEG-PLA-5Fu-^{131}I (200 μCi of ^{131}I). At certain time points, 20 μL of blood samples were collected from the orbital venous plexus of mice. The radioactivity was measured using an automatic gamma counter.

SW620 tumor-bearing mice were intravenously injected with free ^{131}I (200 μCi), Cet-PEG-PLA-^{131}I, and Cet-PEG-PLA-5Fu-^{131}I (200 μCi of ^{131}I), and sacrificed 24 h post injection to detect the biodistribution of nanoparticles. The tumor tissues were collected for the detection of radioactivity. The thyroids of mice were pre-blocked with cold sodium iodide prior to injection with drugs.[29]

In vivo Combined Therapeutic Effects

When the tumor volume reached approximately 100 mm^3, tumor-bearing mice were assigned into six groups (five mice/group) and received saline, Cet-PEG-PLA (50 mg/kg), Cet-PEG-PLA-^{131}I (200 μCi of ^{131}I), Cet-PEG-PLA-5Fu (8 mg/kg of 5Fu), Cet-PEG-PLA-5Fu-^{131}I (8 mg/kg of 5Fu, 200 μCi of ^{131}I), and PEG-PLA-5Fu-^{131}I (8 mg/kg of 5Fu, 200 μCi of ^{131}I) to assess the combined antitumor effects of nanoparticles. The groups received intravenous injections once every 3 days (total of six injections). Tumor size and body weight were measured once every 2 days, and calculated using the following formula: volume (cm^3) = length (L) × width^2 (W^2)/2.

Histopathology and Immunohistochemical Staining

After 20 days of treatment, the mice were sacrificed. The major organs (liver, lungs, and kidneys) and tumor tissues were collected, fixed in 4% formaldehyde, and embedded

in paraffin to prepare the sections (5 μm). Subsequently, the sections were stained with hematoxylin and eosin to examine histological changes. Terminal deoxynucleotidyl transferase UTP nick end labeling (TUNEL) and Ki-67 were also analyzed based on previous literature.[30,31]

Statistical Analysis

All data are representative of three independent experiments and presented as the mean ± standard errors. Statistical analysis was calculated using GraphPad Prism 6.0 (GraphPad Software Inc., USA). Student's *t*-test was employed to compare differences between groups. A p-value <0.05 denoted a statistically significant difference, and a p-value <0.01 was considered highly significant.

Results and Discussion

Characterization of Cet-PEG-PLA -5Fu-^{131}I Nanoparticles

The morphology and size distribution of nanoparticles were detected through TEM and DLS. As shown in Figure 1A, the obtained Cet-PEG-PLA-5Fu-^{131}I nanoparticles showed uniform size distribution with spherical shape. By utilizing DLS, it was found that the mean size of Cet-PEG-PLA -5Fu-^{131}I nanoparticles was approximately 110 nm (Figure 1B), consistent with the results obtained from TEM. Besides, the zeta potential of Cet-PEG-PLA-5Fu-^{131}I was −23.7 mV. FTIR and ^{1}H NMR spectroscopies were used to confirm the synthetic nano-complexes. In FTIR analysis (Figure 1C), an absorption peak at 1,600 cm^{-1} (N-H stretch) was revealed for the successful modification of Cet on the surface of PEG-PLA nanoparticles. In ^{1}H NMR analysis (Figure 1D), a PEG proton peak was obtained at δ 3.70 ppm and a Cet-PEG-PLA nanoparticle proton peak was revealed at δ 4.80 ppm. The radioactive stability of the nanoparticles in the serum and PBS was also determined. As illustrated in Figure 1E, following incubation with Cet-PEG-PLA-^{131}I and Cet-PEG-PLA-5Fu-^{131}I in PBS and serum for 24 h, >80% conservation of total radioactivity was observed. The stability was reduced after 24 h, which may be due to protein interactions in the serum. Meanwhile, the stability of Cet-PEG-PLA nanoparticles was evaluated by measuring the zeta potential (Figure 1F); the results suggested that Cet-PEG-PLA maintained a high level of stability in PBS and serum. In addition, the 5Fu-loading capacity and encapsulation efficiency of Cet-PEG-PLA-5Fu-^{131}I were 15.39 ± 0.27% and 85.62 ± 0.79%, respectively. The radiolabeling yield of Cet-PEG-PLA -5Fu-^{131}I was 42.9 ± 4.1%.

In vitro Release Study

We also sought to determine the properties of PEG-PLA nanoparticles as drug-releasing tools. For this purpose, the in vitro release profiles of 5Fu from Cet-PEG-PLA -5Fu-^{131}I nanoparticles were monitored using PBS with pH 5.0 and 7.4 to simulate the tumor environment and physiological environment, respectively. As shown in Figure 1G, Cet-PEG-PLA-5Fu-^{131}I nanoparticles suggested a sustained release at both pH 5.0 and 7.4. The accumulated release rates of 5Fu from nanoparticles at pH 5.0 and 7.4 within 120 h were 77.67% and 28.35%, respectively. Moreover, the 5Fu release appeared to be more evident in the lower pH condition versus the physical pH environment. This pH-dependent release was beneficial in protecting normal tissues from damage.

Cellular Uptake

The amount of drug taken up by cells plays an important role in the therapeutic effects. ICG, approved for clinical use by the US Food and Drug Administration, is highly biocompatible and has been widely used for tumor cell imaging.[32] In this study, we evaluated the cellular uptake of nanoparticles through encapsulating ICG using a confocal fluorescence microscope (Figure 2). The results showed that the fluorescence intensity of cells treated with Cet-PEG-PLA-ICG was significantly higher than that of cells treated with PEG-PLA-ICG. This indicated that Cet-PEG-PLA-ICG could be readily internalized by SW620 cells compared with PEG-PLA-ICG, and this was attributed to the Cet targeting effect. Cells were pretreated with Cet to block EGFR and further analyze the uptake behavior of Cet-PEG-PLA-ICG. As illustrated, weak fluorescence signals were observed in cells with pre-blocked EGFR prior to incubation with Cet-PEG-PLA-ICG. These results clarified that Cet-PEG-PLA-ICG nanoparticles were able to target cancer cells overexpressing EGFR via the specific recognition between Cet and EGFR. This finding was consistent with a previous report stating that Cet was an efficient tumor-targeting moiety by binding to EGFR excessively expressed on the surface of colorectal cancer cells.[33]

In vitro Cytotoxicity Study

The potential effect of PEG-PLA nanoparticles on the viability of SW620 cells was investigated using the Cell Counting Kit-8 assay. Cet-PEG-PLA did not show marked cytotoxicity against SW620 cells even at a high concentration of 1,000 μg/mL for 24 h (Figure 3A), demonstrating the excellent biocompatibility

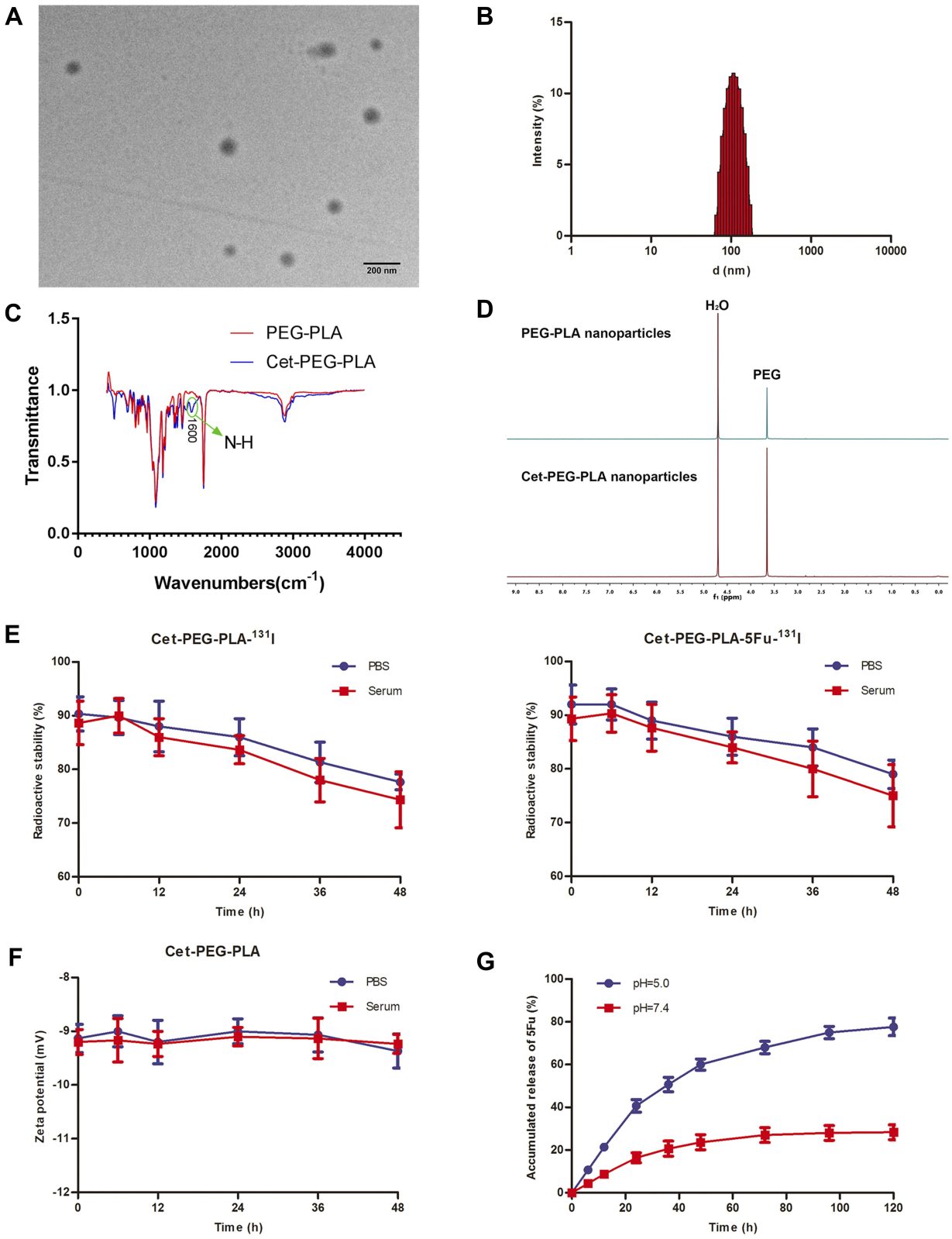

Figure 1 Characterization of Cet-PEG-PLA-5Fu-^{131}I nanoparticles. (**A**) TEM image of Cet-PEG-PLA-5Fu-^{131}I nanoparticles. (**B**) Size distribution of Cet-PEG-PLA -5Fu-^{131}I nanoparticles. (**C**) FTIR analysis. (**D**) ^{1}H NMR spectrum. (**E**) Radioactive stability of Cet-PEG-PLA-^{131}I and Cet-PEG-PLA-5Fu-^{131}I nanoparticles in PBS and serum was determined using a gamma counter. (**F**) Stability of Cet-PEG-PLA in PBS and serum was determined by measuring the zeta potential. (**G**) 5Fu release profiles of Cet-PEG-PLA-5Fu-^{131}I nanoparticles at different pH values.

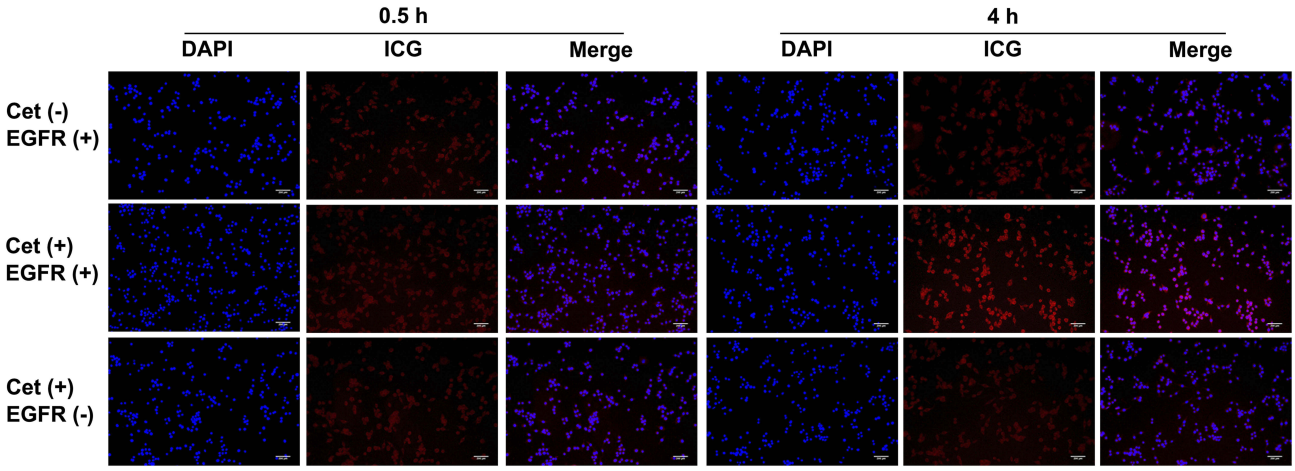

Figure 2 In vitro cellular uptake study. Confocal fluorescence images of SW620 cells incubated with ICG-labeled PEG-PLA and Cet-PEG-PLA for 30 min and 4 h.

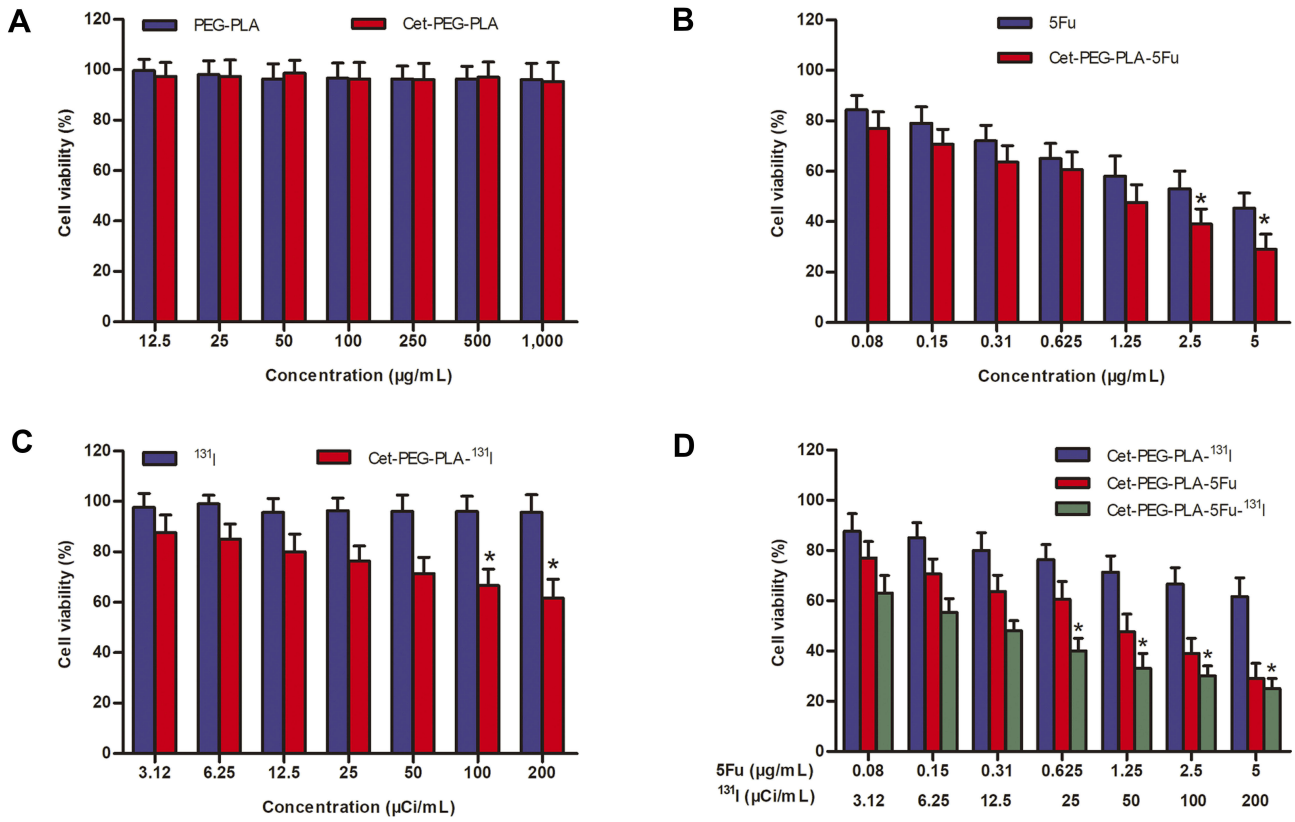

Figure 3 In vitro cell cytotoxicity assay. (**A**) Relative cell viabilities of SW620 cells after treatment with PEG-PLA and Cet-PEG-PLA for 24 h. (**B**) Relative cell viabilities of SW620 cells after treatment with 5Fu and Cet-PEG-PLA-5Fu for 24 h. (**C**) Relative cell viabilities of SW620 cells after treatment with ^{131}I and Cet-PEG-PLA-^{131}I for 24 h. (**D**) Relative cell viabilities of SW620 cells after treatment with Cet-PEG-PLA-5Fu, Cet-PEG-PLA-^{131}I, and Cet-PEG-PLA-5Fu-^{131}I for 24 h. *p<0.05.

of PEG-PLA. The cancer cell-killing ability of 5Fu-loaded and ^{131}I-labeled nanoparticles was subsequently evaluated by incubating SW620 cells with free 5Fu, free ^{131}I, Cet-PEG-PLA -5Fu, Cet-PEG-PLA-^{131}I, or Cet-PEG-PLA-5Fu-^{131}I at different concentrations. It was found that Cet-PEG-PLA-5Fu was more toxic than free 5Fu (Figure 3B), which may be attributed to the increased cellular uptake of 5Fu via Cet-PEG-PLA. Furthermore, there was obvious toxicity of Cet-PEG-PLA--^{131}I compared with free ^{131}I at the same radiation dose (Figure 3C), which may be due to the increased cellular uptake of ^{131}I through PEG-PLA. Furthermore, the combination of radio-chemotherapy (Cet-PEG-PLA-5Fu-^{131}I) resulted in the

most superior cytotoxicity versus monotherapy with Cet-PEG-PLA-5Fu or Cet-PEG-PLA-^{131}I (Figure 3D). Taken together, the results indicated that the combined radio-chemotherapy based on Cet-PEG-PLA-5Fu-^{131}I nanoparticles achieved an enhanced antitumor effect.

Cell Apoptosis

The cytotoxic effects of PEG-PLA-based nanoparticles were further investigated by Annexin-V-propidium iodide apoptosis analysis. As depicted in Figure 4, treatment with Cet-PEG-PLA-5Fu or Cet-PEG-PLA-^{131}I induced early apoptosis in approximately 33% and 21% of cancer cells, respectively. Importantly, Cet-PEG-PLA-5Fu-^{131}I exhibited a distinct apoptotic rate of cells (as high as 44%) in the early phase, suggesting the superior anticancer effects of radio-chemotherapy based on PEG-PLA nanoparticles.

In vivo Circulation in the Blood and Biodistribution

The in vivo behavior of Cet-PEG-PLA-5Fu-^{131}I nanoparticles was evaluated prior to combination treatment. Figures 5A and B show that the half-life of free ^{131}I was very short due to rapid renal filtration. Hence, high doses of ^{131}I are required to achieve certain radiotherapeutic effects, which often result in undesired therapeutic outcomes and damage to normal tissues. As expected, the circulation half-life of Cet-PEG-PLA-5Fu-^{131}I in the blood was longer than that of free ^{131}I, which may be due to the fact that the formulation of nanoparticles could effectively suppress rapid metabolism via enhanced permeability and a retention effect.[34] Consequently, the adverse effects caused by ^{131}I could be reduced.

The detailed biodistribution of free ^{131}I, Cet-PEG-PLA-^{131}I, and Cet-PEG-PLA-5Fu-^{131}I nanoparticles in xenograft mice was examined 24 h post injection (Figure 5C). The accumulation of Cet-PEG-PLA-5Fu-^{131}I in the tumor was approximately three-fold higher than that of free ^{131}I, possibly caused by the active tumor-targeting ability of Cet-PEG-PLA-5Fu-^{131}I nanoparticles. Of note, the radioactivity levels in other organs of mice injected with Cet-PEG-PLA-5Fu-^{131}I were <5% ID/g, except for the liver due to the strong liver first-pass effect of drugs. Collectively, these results indicate that Cet-PEG-PLA-5Fu-^{131}I nanoparticles have a conspicuous active tumor-targeting ability.

In vivo Combination Therapy Based on PEG-PLA Nanoparticles

We successfully established the xenograft mice model to investigate the antitumor activity of PEG-PLA-based nanoparticles in vivo. Monotherapy with Cet-PEG-PLA-5Fu (chemotherapy) or Cet-PEG-PLA-^{131}I (radiotherapy) inhibited

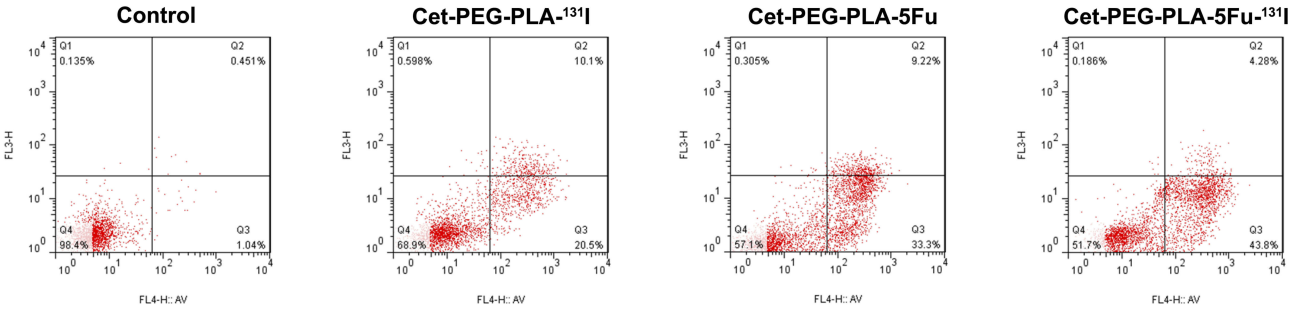

Figure 4 Cell apoptosis induced by PEG-PLA nanoparticles. Flow cytometric analysis of SW620 cells treated with nanoparticles for 24 h.

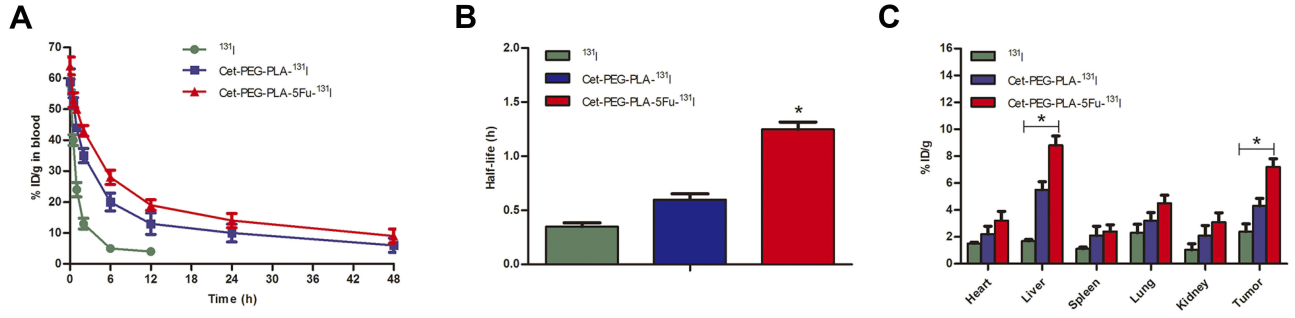

Figure 5 In vivo circulation in the blood and biodistribution. (**A**) Circulation in the blood and (**B**) half-life of ^{131}I, Cet-PEG-PLA-^{131}I, and Cet-PEG-PLA-5Fu-^{131}I. (**C**) Biodistribution of ^{131}I, Cet-PEG-PLA-^{131}I, and Cet-PEG-PLA-5Fu-^{131}I measured 24 h post injection. *p<0.05.

tumor growth slightly compared with saline or blank Cet-PEG-PLA treatment (Figures 6A and B). Moreover, the combination treatment of Cet-PEG-PLA-5Fu-^{131}I markedly suppressed tumor growth, revealing the significantly enhanced effects of combination therapy. Notably, treatment with Cet-PEG-PLA-5Fu-^{131}I exhibited stronger suppressive activity compared with PEG-PLA-5Fu-^{131}I. This is likely attributed to the fact that Cet could promote EGFR-mediated tumor-targeted accumulation and prolong circulation in the blood, thereby leading to improved therapeutic outcomes. The body weight of the mice was also monitored to further investigate whether these treatments would stimulate toxicity. As expected, the body weights of the mice in the treated groups were approximately equal to those reported in the control group. There was no loss of body weight or other serious toxic effects (Figure 6C), demonstrating the good biocompatibility and reliable safety of PEG-PLA-based nanoparticles. Collectively, combined chemo-radiotherapy using PEG-functionalized PLA nanoparticles as the nanocarrier offers excellent advantages in the treatment of cancer with improved therapeutic efficacy.

Histological and Immunohistochemical Analyses

Histological tissue slides of tumors and major tissues (liver, lungs, and kidneys) after 20 days of treatment were prepared (Figure 7) to further investigate the antitumor effects of PEG-PLA-based nanoparticles. Compared with saline or blank nanoparticles, Cet-PEG-PLA-5Fu and Cet-PEG-PLA-^{131}I exhibited similar tumor-inhibition ability. However, treatment with Cet-PEG-PLA-5Fu-^{131}I showed more tumor necrosis than monotherapy with Cet-PEG-PLA-5Fu or Cet-PEG-PLA-^{131}I, suggesting the stronger tumor suppression ability of combined therapy based on PEG-PLA nanoparticles. On the other hand, there were no obvious changes observed in the major organs. The tumor-inhibition capability of PEG-PLA nanoparticles was also assessed by immunohistochemical analysis. Figure 7 shows that the protein expression of Ki-67 (a crucial tumor proliferation marker) was markedly decreased following treatment with Cet-PEG-PLA-5Fu-^{131}I versus that recorded after treatment with Cet-PEG-PLA-5Fu or Cet-PEG-PLA-^{131}I alone. This finding indicates that Cet-PEG-PLA-5Fu-^{131}I nanoparticles exert better antitumor effects. Moreover, the rate of tumor cell apoptosis was also analyzed using the TUNEL assay. The results showed that Cet-PEG-PLA-5Fu and Cet-PEG-PLA-^{131}I induced tumor cell apoptosis to a certain extent. In contrast, combined treatment with Cet-PEG-PLA-5Fu-^{131}I exhibited the highest rate of apoptotic tumor cells, manifesting an efficient inhibition of tumor growth by Cet-PEG-PLA-5Fu-^{131}I, in line with the above results. Overall, Cet-PEG-PLA-5Fu-^{131}I nanoparticles could inhibit the proliferation of cancer cells, repress tumor growth, and trigger tumor cell apoptosis, thereby resulting in enhanced antitumor efficacy.

Conclusions

In summary, we have successfully developed a multifunctional drug delivery system for tumor-targeted treatment. The prepared Cet-PEG-PLA-5Fu-^{131}I nanoparticles possessed the following characteristics: (1) sustained 5Fu release under the intracellular pH condition; and (2) high cellular uptake by Cet decoration. Moreover, by tracking the radioactive levels of Cet-PEG-PLA-5Fu-^{131}I, we showed that these nanoparticles had a prolonged circulation time in the blood and efficient tumor-targeted accumulation. Importantly, Cet-PEG-PLA-5Fu-^{131}I showed a distinct combined effect on the inhibition of tumor growth, which was superior to monotherapy with Cet-PEG-PLA-5Fu or Cet-PEG-PLA-^{131}I. Through combined chemotherapy and radiotherapy, Cet-PEG-PLA-5Fu-^{131}I showed obvious therapeutic advantages

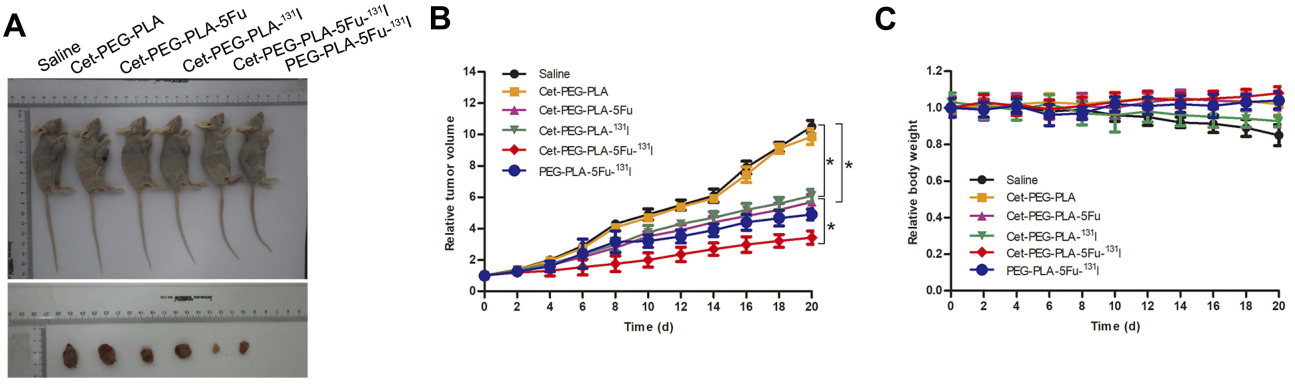

Figure 6 In vivo combined therapy based on PEG-PLA nanoparticles. (**A**) Tumor volume, (**B**) tumor growth, and (**C**) body weight of mice receiving different treatments. *p<0.05.

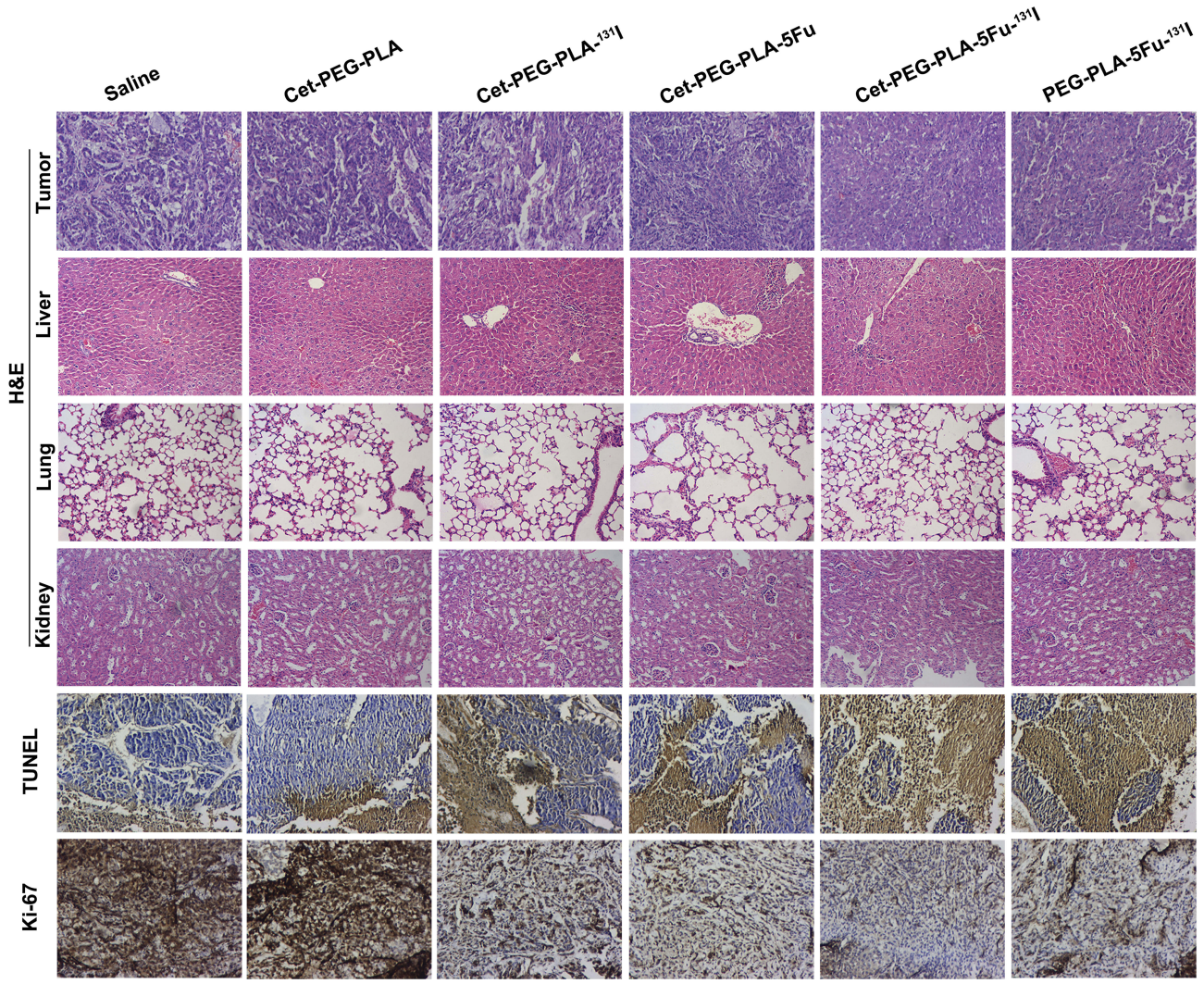

Figure 7 Histological analysis of in vivo combined therapy. Micrograph of H&E-, TUNEL-, and Ki-67-stained tumor slices flensed from the mice 20 days after treatment.

over monotherapy. The results highlight the promising potential of Cet-PEG-PLA-5Fu-^{131}I nanoparticles for combined radiochemotherapy in colorectal cancer.

Funding

This project was supported by the National Natural Science Youth Foundation of China (No. 81601604), the Natural Science Youth Foundation of Jiangsu (No. BK20161070), the Fifteenth Batch High-level Talents Project of "Six Talent Peaks" in Jiangsu Province (No. WSW-049), the Key Project of Natural Science Foundation of China (No. 51832001), and the talents program of Jiangsu Cancer Hospital (No. YC201809).

Disclosure

The authors report no conflicts of interest in this work.

References

1. Hadjipetrou A, Anyfantakis D, Galanakis CG, Kastanakis M, Kastanakis S. Colorectal cancer, screening and primary care: a mini literature review. *World J Gastroenterol*. 2017;23(33):6049–6058. doi:10.3748/wjg.v23.i33.6049
2. Parkin DM, Bray F, Ferlay J, Pisani P. Global cancer statistics, 2002. *CA Cancer J Clin*. 2005;55(2):74–108. doi:10.3322/canjclin.55.2.74
3. Mishra J, Drummond J, Quazi SH, et al. Prospective of colon cancer treatments and scope for combinatorial approach to enhanced cancer cell apoptosis. *Crit Rev Oncol Hematol*. 2013;86(3):232–250. doi:10.1016/j.critrevonc.2012.09.014
4. Wang CL, Wu WY, Lou HM, et al. Analysis of symptom clusters in Chinese cervical cancer patients undergoing radiotherapy, chemoradiotherapy, or postoperative chemoradiotherapy. *Eur J Gynaecol Oncol*. 2017;38(3):398–403.
5. Parve S, Aliakberova GI, Gylmanov AA, Abdulganieva DI. Role of exogenous phosphocreatine in chemotherapy-induced cardiomyopathy. *Rev Cardiovasc Med*. 2017;18(2):82–87.
6. Pérez-Herrero E, Fernández-Medarde A. Advanced targeted therapies in cancer: drug nanocarriers, the future of chemotherapy. *Eur J Pharm Biopharm*. 2015;93:52–79. doi:10.1016/j.ejpb.2015.03.018

7. Bradley JD, Paulus R, Komaki R, et al. Standard-dose versus high-dose conformal radiotherapy with concurrent and consolidation carboplatin plus paclitaxel with or without cetuximab for patients with stage IIIA or IIIB non-small-cell lung cancer (RTOG 0617): a randomised, two-by-two factorial phase 3 study. *Lancet Oncol*. 2015;16(2):187–199. doi:10.1016/S1470-2045(14)71207-0
8. Maiti D, Chao Y, Dong Z, et al. Development of a thermosensitive protein conjugated nanogel for enhanced radio-chemotherapy of cancer. *Nanoscale*. 2018;10(29):13976–13985. doi:10.1039/C8NR03986K
9. Hathout L, Ellingson B, Pope W. Modeling the efficacy of the extent of surgical resection in the setting of radiation therapy for glioblastoma. *Cancer Sci*. 2016;107(8):1110–1116. doi:10.1111/cas.12979
10. Song X, Liang C, Feng L, Yang K, Liu Z. Iodine-131-labeled, transferrin-capped polypyrrole nanoparticles for tumor-targeted synergistic photothermal-radioisotope therapy. *Biomater Sci*. 2017;5(9):1828–1835. doi:10.1039/C7BM00409E
11. Thomas AM, Kapanen AI, Hare JI, et al. Development of a liposomal nanoparticle formulation of 5-fluorouracil for parenteral administration: formulation design, pharmacokinetics and efficacy. *J Control Release*. 2011;150(2):212–219. doi:10.1016/j.jconrel.2010.11.018
12. Pretel E, Arias JL, Cabeza L, et al. Development of biomedical 5-fluorouracil nanoplatforms for colon cancer chemotherapy: influence of process and formulation parameters. *Int J Pharm*. 2017;530(1–2):155–164. doi:10.1016/j.ijpharm.2017.07.055
13. Yang X, Grailer JJ, Rowland IJ, et al. Multifunctional stable and pH-responsive polymer vesicles formed by heterofunctional triblock copolymer for targeted anticancer drug delivery and ultrasensitive MR imaging. *ACS Nano*. 2010;4(11):6805–6817. doi:10.1021/nn101670k
14. Snigdha K, Singh BK, Mehta AS, Tewari RP, Dutta PK. Self-assembling N-(9-Fluorenylmethoxycarbonyl)-L-Phenylalanine hydrogel as novel drug carrier. *Int J Biol Macromol*. 2016;93:1639–1646. doi:10.1016/j.ijbiomac.2016.04.072
15. Wang Z, Duan Y, Duan Y. Application of polydopamine in tumor targeted drug delivery system and its drug release behavior. *J Control Release*. 2018;290:56–74. doi:10.1016/j.jconrel.2018.10.009
16. Dai Z, Ma H, Tian L, et al. Construction of a multifunctional nanoprobe for tumor-targeted time-gated luminescence and magnetic resonance in vitro and in vivo. *Nanoscale*. 2018;10(24):11597–11603. doi:10.1039/C8NR03085E
17. Gabizon A, Shmeeda H, Barenholz Y. Pharmacokinetics of pegylated liposomal doxorubicin: review of animal and human studies. *Clin Pharmacokinet*. 2003;42(5):419–436. doi:10.2165/00003088-200342050-00002
18. Allen TM, Cullis PR. Drug delivery systems: entering the mainstream. *Science*. 2004;303(5665):1818–1822.
19. Roskoski R Jr. Small molecule inhibitors targeting the EGFR/ErbB family of protein-tyrosine kinases in human cancers. *Pharmacol Res*. 2019;139:395–411. doi:10.1016/j.phrs.2018.11.014
20. Yun S, Kwak Y, Nam SK, et al. Ligand-independent epidermal growth factor receptor overexpression correlates with poor prognosis in colorectal cancer. *Cancer Res Treat*. 2018;50(4):1351–1361. doi:10.4143/crt.2017.487
21. Wang JK, Zhou YY, Guo SJ, et al. Cetuximab conjugated and doxorubicin loaded silica nanoparticles for tumor-targeting and tumor microenvironment responsive binary drug delivery of liver cancer therapy. *Mater Sci Eng C Mater Biol Appl*. 2017;76:944–950. doi:10.1016/j.msec.2017.03.131
22. Thauvin C, Schwarz B, Delie F, Allémann E. Functionalized PLA polymers to control loading and/or release properties of drug-loaded nanoparticles. *Int J Pharm*. 2018;548(2):771–777. doi:10.1016/j.ijpharm.2017.11.001
23. Leelakanok N, Geary S, Salem A. Fabrication and use of poly(D,L-lactide-co-glycolide)-based formulations designed for modified release of 5-fluorouracil. *J Pharm Sci*. 2018;107(2):513–528. doi:10.1016/j.xphs.2017.10.012
24. Feng SS, Dong Y. Nanoparticles of poly(D,L-lactide)/methoxy poly(ethylene glycol)-poly(D,L-lactide) blends for controlled release of paclitaxel. *J Biomed Mater Res A*. 2006;78(1):12–19. doi:10.1002/jbm.a.30684
25. Xiao RZ, Zeng ZW, Zhou GL, Wang JJ, Li FZ, Wang AM. Recent advances in PEG-PLA block copolymer nanoparticles. *Int J Nanomedicine*. 2010;5:1057–1065. doi:10.2147/IJN.S14912
26. Gong J, Chen M, Zheng Y, Wang S, Wang Y. Polymeric micelles drug delivery system in oncology. *J Control Release*. 2012;159(3):321–323. doi:10.1016/j.jconrel.2011.12.012
27. Li Z, Wang B, Zhang Z, et al. Radionuclide imaging-guided chemo-radioisotope synergistic therapy using I-131 labeled polydopamine multifunctional nanocarrier. *Mol Ther*. 2018;26(5):1385–1393. doi:10.1016/j.ymthe.2018.02.019
28. Filippi M, Garello F, Pasquino C, et al. Indocyanine green labeling for optical and photoacoustic imaging of mesenchymal stem cells after in vivo transplantation. *J Biophotonics*. 2019;12(5):e201800035. doi:10.1002/jbio.2019.12.issue-5
29. Gao J, Fang L, Sun D, et al. (131)I-labeled and DOX-loaded multifunctional nanoliposomes for radiotherapy and chemotherapy in brain gliomas. *Brain Res*. 2016;S0006–8993(16):30833–30842.
30. Mangiavini L, Schipani E. TUNEL assay on skeletal tissue sections to detect cell death. *Methods Mol Biol*. 2014;1130:245–248.
31. Wang Z, Zeng X, Chen R, Chen Z. Ki-67 index and percentage of sarcomatoid differentiation were two independent prognostic predictors in sarcomatoid renal cell carcinoma. *Cancer Manag Res*. 2018;10:5339–5347. doi:10.2147/CMAR
32. Kanazaki K, Sano K, Makino A, Homma T, Ono M, Saji H. Polyoxazoline multivalently conjugated with indocyanine green for sensitive in vivo photoacoustic imaging of tumors. *Sci Rep*. 2016;6(1):33798. doi:10.1038/srep33798
33. Della Corte CM, Ciaramella V, Cardone C, et al. Antitumor efficacy of dual blockade of EGFR signaling by osimertinib in combination with selumetinib or cetuximab in activated EGFR human NCLC tumor models. *J Thorac Oncol*. 2018;13(6):810–820. doi:10.1016/j.jtho.2018.02.025
34. Kirpotin DB, Drummond DC, Shao Y, et al. Antibody targeting of long-circulating lipidic nanoparticles does not increase tumor localization but does increase internalization in animal models. *Cancer Res*. 2006;66(13):6732–6740. doi:10.1158/0008-5472.CAN-05-4199